[CANCER RESEARCH 62, 3331–3334, June 15, 2002]

Advances in Brief

3-Deoxy-3-[^{18}F]Fluorothymidine-Positron Emission Tomography for Noninvasive Assessment of Proliferation in Pulmonary Nodules

Andreas K. Buck,[1] Holger Schirrmeister, Martin Hetzel, Mareike von der Heide, Gisela Halter, Gerhard Glatting, Torsten Mattfeldt, Florian Liewald, Sven N. Reske, and Bernd Neumaier

Departments of Nuclear Medicine [A. K. B., H. S., M. v. d. H., G. G., S. N. R., B. N.], Internal Medicine II [M. H.], Thoracic Surgery [G. H., F. L.], and Pathology [T. M.], Universit of Ulm, D-89081 Ulm, Germany

Abstract

We investigated whether uptake of the thymidine analogue 3-deoxy-3-[^{18}F]fluorothymidine ([^{18}F]FLT) reflects proliferation in solitary pulmonary nodules (SPNs). Thirty patients with SPNs were prospectively examined with positron emission tomography. Standardized uptake values were calculated for quantification of FLT uptake. Histopathology revealed 22 malignant and 8 benign lesions. Proliferation was evaluated by Ki-67 immunostaining and showed a mean proliferation fraction of 30.9% (range, 1–65%) in malignant SPNs and <5% in benign lesions. Linear regression analysis indicated a significant correlation between FLT-standardized uptake values and proliferative activity ($P < 0.0001$; $r = 0.87$). FLT uptake was specific for malignant lesions and may be used for differential diagnosis of SPNs, assessment of proliferation, and estimation of prognosis.

Introduction

Evaluation of SPNs[2] remains one of the most common diagnostic problems in daily clinical practice (1). Only half of the resected lesions are related to malignant disease (1), and many of the nonmalignant lesions represent inflammatory processes (2). PET using the glucose analogue FDG enables noninvasive differentiation between benign and malignant lesions because glucose consumption is elevated in malignant tumors (3). FDG uptake, however, is not specific for malignancies because false positive findings were also reported in inflammation, muscle activity, or sarcoidosis (2). A study in patients with elevated FDG uptake in pancreatic tumors indicated that determination of the proliferation rate clearly differentiated cancer from inflammation (4). Recently, Shields *et al.* (5) developed the new PET tracer FLT for noninvasive measurement of tumor proliferation. This thymidine analogue was reported to accumulate in proliferating cells after intracellular trapping because of phosphorylation by thymidine kinase 1 (6). This first study in humans was conducted to evaluate the correlation between [^{18}F]FLT uptake and the proliferation rate in SPNs.

Materials and Methods

Patients. This prospective study consisted of 30 patients (20 men and 10 women) with a mean age of 61.9 ± 6.8 years (range, 37–88 years). Patients were included when pulmonary nodules on CT with and without contrast enhancement were suspicious for a malignant tumor. None of the patients had prior surgery, chemotherapy, or radiation therapy. Nineteen patients had resective surgery up to 10 days after FLT-PET. Core biopsy specimens were used to evaluate the proliferation in the other 11 patients. All patients gave written consent to participate in this study, which was approved by the local ethical committee.

Histopathology. Histopathological examination of the resected specimens revealed 22 malignant tumors [16 NSCLC, 1 small cell lung cancer, 1 non-Hodgkin's lymphoma, and pulmonary metastases in 4 patients (1 colorectal cancer, 2 renal cell carcinoma, and 1 osteosarcoma)] and 8 benign tumors (1 bronchopulmonary chondroma, 3 bronchiolitis, 1 tuberculoma, 1 focal fibrosis, and 2 undefined tumors; malignancy excluded by clinical course).

Immunostaining. A standard peroxidase-conjugated streptavidin-biotin complex method was used (DAKO Diagnostika, Hamburg, Germany), and 3,3′-diaminobenzidine (Sigma-Aldrich, Deisenhofen, Germany) served as chromogen (4). Briefly, formalin-fixed, paraffin-embedded sections (5 μm) of resected specimens were dewaxed, rehydrated, and then microwaved in 0.01 M citrate buffer for 30 min. For immunostaining, MIB-1 antibody (Dianova, Hamburg, Germany), a monoclonal murine antibody specific for human nuclear antigen Ki-67, was used as the primary antibody in a 1:500 dilution. Sections were lightly counterstained with hematoxylin. The primary antibody was omitted on sections used as negative controls. Sections obtained from highly proliferating lymph node tissue of a reference patient who was not included in our series served as a positive control for proliferating cells. An evaluation of MIB-1 immunostaining was carried out in an area with high cellularity. All epithelial cells with nuclear staining of any intensity were defined as positive. Proliferative activity was described as the percentage of MIB-1-stained nuclei.

Morphometry. Histopathological slides were scored by a pathologist experienced in this field who was blinded to the patients' clinical data. The fraction of stained nucleus profile per total number of nucleus profiles was estimated by counting 600 nuclei/slide and three slides/case. For this purpose, the computer assisted imaging system Optimas 6.2 (Media Cybernetics, Inc., Silver Spring, MD) was used. Slides were analyzed by light microscopy, and three representative images of each slide were transferred to the computer frame by a video camera.

[^{18}F]FLT Synthesis. [^{18}F]FLT was produced via benzoyl-protected anhydrothymidine according to the method reported by Machulla (7). Radiosynthesis was carried out remotely and automatically in a PET tracer synthesizer from Nuclear Interface (Münster, Germany). [^{18}F]Fluoride was produced via the ^{18}O(p,n) ^{18}F nuclear reaction by bombardment of isotopically enriched [^{18}O]water with an 18 MeV proton beam at the Cyclone 18/9 cyclotron (IBA, Louvaine-la-Neuve, Belgium). After recovery of [^{18}O]water using a QMA cartridge (Waters, Milford, MA), [^{18}F]fluoride was eluted with 360 μl of K_2CO_3 solution (3.3 mg K_2CO_3). Twenty mg of Kryptofix 2.2.2 (Merck, Darmstadt, Germany) in 0.7 ml of acetonitrile was added, and the cryptate of [^{18}F]fluoride and potassium carbonate was evaporated to dryness. The evaporation step was repeated with 1 ml of acetonitrile to remove any traces of moisture. Then a solution of 10 mg of 5′-benzoyl-3′,2-anhydrothymidine in 1 ml of DMSO was added to the dry cryptate, and the resulting solution kept at 160°C for 10 min. Removal of the benzoyl-protecting group was achieved by hydrolysis with 1% 350-μl 1 M NaOH and heating it to 55°C for 10 min. The hydrolysate was transferred through an Alumina N (Waters) to retard unreacted [^{18}F]fluoride. Subsequently, [^{18}F]FLT was purified using preparative high-performance liquid chromatography. For the separation of [^{18}F]FLT, a C-18 column (Phenomenex; Luna 5 μ, 250 × 10 mm) was used and eluted with isotonic sodium chloride solution and ethanol (90/10, v/v) at a flow rate

Received 2/15/02; accepted 5/1/02.
The costs of publication of this article were defrayed in part by the payment of page charges. This article must therefore be hereby marked *advertisement* in accordance with 18 U.S.C. Section 1734 solely to indicate this fact.
[1] To whom requests for reprints should be addressed, at Universit of Ulm, Robert-Koch-Strasse 8, D-89081 Ulm, Germany. Phone: 0731-500-24504; Fax: 0731-500-24503; E-mail: andreas.buck@medizin.uni-ulm.de.
[2] The abbreviations used are: SPN, solitary pulmonary nodule; PET, positron emission tomography; FDG, 2-[^{18}F]fluoro-2-deoxy-D-glucose; FLT, 3-deoxy-3′-fluorothymidine; NSCLC, non-small cell lung cancer; SUV, standardized uptake value; CT, computed tomography.

of 5 ml/min. Retention time of [^{18}F]FLT was 10 min. It was separated from other ^{18}F impurities, mainly [^{18}F]fluoride. Finally the collected product was sterile filtered through a 0.2 μm Sterifix filter (Braun, Melsungen, Germany).

FLT-PET Imaging. PET was performed using a high-resolution full ring scanner (ECAT Exact; Siemens/CTI, Knoxville, TN), which produces 47 contiguous slices/bed position. Axial field of view is 15.5 cm/bed position. Patients fasted for at least 6 h before undergoing PET. Static emission scans were started 45 min after injection of 265–370 MBq of [^{18}F]FLT (mean, 334 MBq). The acquisition time was 10 min/bed position for emission scanning. Eight-min transmission scans with a germanium-68/gallium-68 ring source were obtained for attenuation correction. Five bed positions covered a field of view of 77.5 cm in each patient. Images were reconstructed using an iterative reconstruction algorithm (8). For SUV calculation, circular regions of interest were drawn around the area with focally increased pulmonary FLT uptake.

Data Analysis. Data are presented as mean, median, range, and SD. Amounts of Ki-67 positive cells and FLT-SUVs were compared using linear regression analysis. Differences were considered statistically significant when $P < 0.05$.

Results

FLT-PET. Mean [^{18}F]FLT uptake (FLT-SUV) in SPN was 2.8 (median, 3.1; range, 0–6.4; and SD, 1.8), and the mean maximum FLT-SUV was 4.2 (median, 4.4; range, 0–10.4; and SD, 2.9; Table 1). NSCLC was the predominant tumor entity. With the exception of one carcinoma *in situ* (patient 16) and a highly differentiated large cell NSCLC (patient 6) with a low proliferation index of 10%, FLT-SUV was markedly increased in NSCLC (Fig. 1). On the basis of the expert qualitative review, sensitivity of FLT-PET is 86%. Using a cutoff level of $SUV_{max} = 1.5$, sensitivity of FLT-PET is 77%. Mean FLT-SUV was 3.5 (median, 3.2; range, 0–6.4; and SD, 1.7) in NSCLC, and the mean maximum FLT-SUV was 5.2 (median, 4.7; range, 0–10.4; and SD, 2.6). All benign tumors presented without [^{18}F]FLT uptake. Hence, SUVs were not calculated in these lesions.

Pulmonary metastases presented without [^{18}F]FLT uptake in one patient with recurrent colorectal cancer. A NSCLC (patient 12) and a pulmonary metastasis from osteosarcoma (patient 22) showed a weak but easily detectable [^{18}F]FLT uptake (Table 1).

Ki-67 Immunohistochemistry. All malignant tissue specimens contained Ki-67 positive cells. Stained nuclei mainly belonged to epithelial cells, and a very small portion to inflammatory cells. Ki-67 positivity ranged from 1 to 70% of sampled epithelial nucleus profiles (Table 1). The mean proliferation fraction in malignant SPNs was 30.9% (median, 33.5%; range, 1–70%; and SD, 18.9%), and in NSCLC, it was 33% (median, 35%; range, 10–70%; and SD, 6.5%).

More than 40% of stained nuclei was present in 8 malignant lesions. The mean proliferation fraction was 15% (range, 0–35%) in lung metastases. Only 1 benign nodule contained Ki-67 positive cells (patient 25 with solitary tuberculoma, Ki-67 index, 5%). In control sections in which the primary antibody was omitted, no positive nuclear staining was present.

Correlation between Proliferative Activity and FLT Uptake. Immunoreactivity to Ki-67 antigen was present in all malignant nodules. Linear regression analysis indicated a highly significant correlation between FLT-SUV and Ki-67 index in the malignant lesions ($P < 0.0001$; $r = 0.87$; Fig. 2). In benign tumors, maximum proliferation rate was <5% and no FLT uptake was visible.

Discussion

Our data indicate that [^{18}F]FLT uptake reflects proliferative activity as determined by Ki-67 immunostaining. This correlation was highly significant with a correlation coefficient of 0.87 ($P < 0.0001$). FLT uptake was exclusively present in malignant lesions. Benign lesions showed a mean proliferation fraction < 5% and did not accumulate FLT. FLT-PET was false negative in one well-differentiated large cell NSCLC, with a proliferation fraction of 10% and in lung metastases of colorectal cancer in another patient. Proliferative index was as low as 12% in these metastases. These false-negative findings are probably explained by a low cell turnover and concomitantly lower thymidine kinase activity, but other mechanisms such as competition to endogenous thymidine kinase substrates cannot be ruled out. A carcinoma *in situ* with a proliferation rate of 35% was also not visible.

Table 1 *Patient and tumor characteristics*

Patient no.	Age	Sex	Histopathology	TNM	SUV-FLT mean	SUV-FLT max	Ki-67 index
1	57	F	NSCLC	$T_1N_1M_0$	5.63	8.7	65%
2	53	M	NSCLC	$T_2N_1M_0$	4.02	5	41%
3	77	F	NSCLC	$T_2N_1M_0$	3.98	5.3	43%
4	71	F	NSCLC	$T_2N_1M_0$	2.9	4.4	35%
5	75	M	NSCLC	$T_2bN_0M_0$	3.06	5.7	54%
6	53	F	NSCLC	$T_2N_1M_0$	Neg.	Neg.	10%
7	61	M	NSCLC	$T_3N_0M_0$	4.89	6.8	45%
8	66	M	NSCLC	$T_1N_0M_0$	3.24	4.7	26%
9	76	M	NSCLC	$T_4N_2M_0$	3.05	5.2	35%
10	55	M	NSCLC	T_2N_2Mx	3.88	5.6	40%
11	62	F	NSCLC	TxN_0M_0	2.26	3.3	10%
12	55	M	NSCLC	$T_1N_1M_0$	1.11	1.3	12%
13	51	F	NSCLC	$T_2N_2M_1$	3.64	6.10	43%
14	60	M	NSCLC	$T_4N_1M_0$	5.62	8.2	40%
15	56	F	NSCLC	$T_3N_3M_0$	6.38	10.4	70%
16	67	M	NSCLC (carcinoma *in situ*)	$T_1N_0M_0$	Neg.	Neg.	32%
17	66	M	SCLC	$T_4N_2M_0$	1.69	2.4	20%
18	50	M	Non-Hodgkin's lymphoma	$T_2N_0M_0$	2.53	4.2	12%
19	68	M	Colorectal cancer, pulmonary met	$rTxN_0M_1$	Neg.	Neg.	12%
20	51	M	Renal cell carcinoma, pulmonary met	$rTxN_0M_1$	2.07	3.4	23%
21	65	M	Renal cell carcinoma, pulmonary met	$rTxN_0M_1$	1.32	1.9	10%
22	37	F	Osteosarcoma, pulmonary met	TxN_0M_1	0.816	1	1%
23	75	M	Bronchiolitis	-	Neg.	Neg.	0%
24	76	M	2×3 cm nodule, clinical course indicated benign lesion	-	Neg.	Neg.	0%
25	51	F	Tuberculoma	-	Neg.	Neg.	5%
26	59	M	Bronchiolitis	-	Neg.	Neg.	0%
27	69	M	Bronchiolitis	-	Neg.	Neg.	0%
28	67	M	1×2 cm nodule, clinical course indicated benign lesion	-	Neg.	Neg.	0%
29	55	F	Fibroma	-	Neg.	Neg.	0%
30	56	M	Bronchopulmonary chondroma	-	Neg.	Neg.	0%

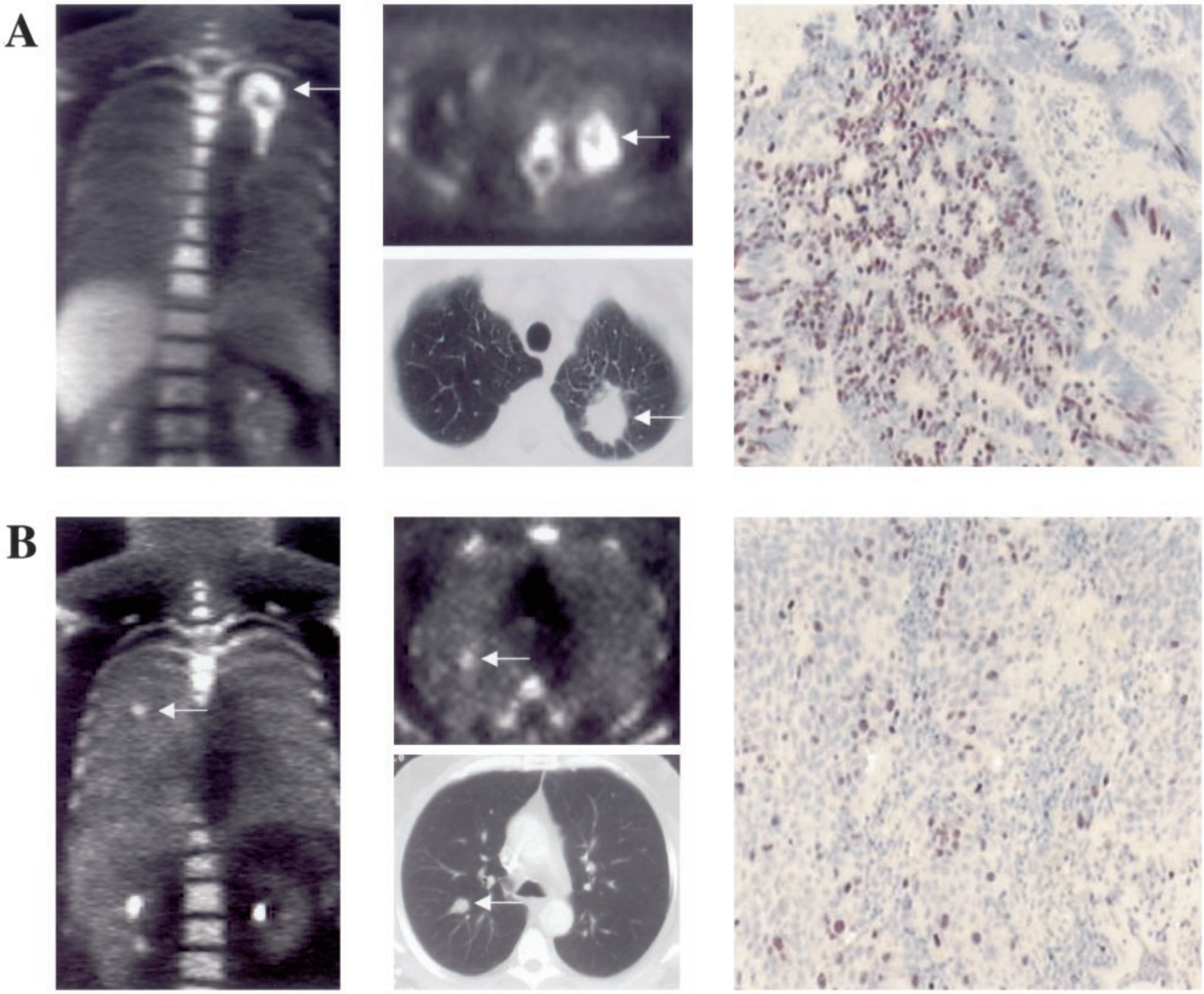

Fig. 1. *A*, FLT-PET of patient 15 with NSCLC with high proliferation fraction and increased FLT uptake (SUV, 6.38) in the tumor margin (70% stained nuclei in the tumor margin, *right*). *Middle*, transverse sections of PET and spiral CT. *B*, patient 12 with a low proliferating NSCLC (25% stained nuclei, *right*). FLT-PET (*left*) shows moderate FLT-uptake (SUV, 1.11). *Middle*, corresponding transverse sections of the spiral CT.

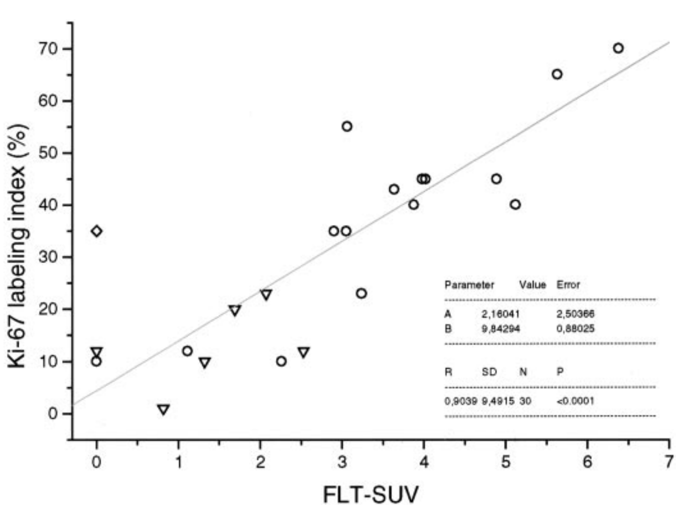

Fig. 2. Linear regression analysis demonstrates a significant correlation between proliferative fraction and FLT uptake in SPN. ○, NSCLC; ◇, patient 16 with a carcinoma *in situ* (NSCLC) negative on FLT-PET; ▽, other malignant lesions.

This was presumably caused by partial volume effects because lesions < 0.5 cm may generally be missed on PET.

Despite the perfect specificity of 100%, FLT-PET showed a lack of sensitivity in a highly differentiated lung tumor and in metastases from colorectal cancer. That means, in effect, that histopathological examination for evaluation cannot be omitted when SPNs do not accumulate [^{18}F]FLT. It has to be mentioned that our series consisted exclusively of untreated patients with suspicious lung lesions. The 100% rate of specificity and the 86% rate of sensitivity may be different for the evaluation of patients who have undergone treatment.

The proliferation rate is currently discussed as a prognostic marker (9, 10). For example, patients with increased tumor proliferation as determined by the thymidine labeling index or Ki-67 immunostaining showed decreased survival in NSCLC (11, 12). However, in another series, Ki-67 staining in stage I NSCLC was not a significant predictor of outcome (13). Commonly, proliferation cannot be measured in the entire tumor but only in a small, probably representative portion. Because of sampling errors, this method is naturally not precise. Therefore, noninvasive determination of the proliferation of the entire tumor should be helpful for a more exact estimation of the prognosis with FLT-PET.

Recently, a significant correlation between FDG uptake and proliferation in NSCLC was suggested (14, 15). However, the correlation coefficient of $r = 0.74$ indicated that tumoral FDG uptake originated from additional mechanisms such as expression of glucose transporters (16) rather than from proliferation alone. Several authors reported that high FDG uptake in NSCLC was associated with decreased survival (17–19). Correlation to proliferative activity has not been assessed in these studies. Compared with FDG-PET studies, the number of patients is relatively small in our series. The correlation coefficient and the perfect specificity may not hold up in a larger series. However, the greater correlation coefficient of 0.9 suggested that FLT reflects proliferation better than FDG. The high tracer uptake observed in the bone marrow supports the concept of a preferential tracer accumulation in proliferating cells (Fig. 1).

In summary, [^{18}F]FLT may be used for noninvasive assessment of proliferation in SPN, which was a typical feature of malignant lesions. Furthermore, a better prediction of prognosis and improved selection of the appropriate therapeutic regimen seems feasible.

References

1. Svensen, S., Viggiano, R., Midthun, D., Müller, N., Sherrick, A., Ymashita, K., Naidich, D., Patz, E., Hartman, T., Muhm, J., and Weaver, A. Lung nodule enhancement at CT: multicenter study. Radiology, *214:* 73–80, 2000.
2. Shreve, P., Anzai, Y., and Wahl, R. Pitfalls in oncologic diagnosis with FDG PET imaging: physiologic and benign variants. Radiographics, *19:* 61–77, 1999.
3. Kalff, V., Hicks, R. J., MacManus, M. P., Binns, D. S., McKenzie, A. F., Ware, R. E., Hogg, A., and Ball, D. L. Clinical impact of (18)F fluorodeoxyglucose positron emission tomography in patients with non-small cell lung cancer: a prospective study. J. Clin. Oncol., *19:* 111–118, 2001.
4. Buck, A. C., Schirrmeister, H. H., Guhlmann, C. A., Diederichs, C. G., Shen, C., Buchmann, I., Kotzerke, J., Birk, D., Mattfeldt, T., and Reske, S. N. Ki-67 immunostaining in pancreatic cancer and chronic active pancreatitis: does *in vivo* FDG uptake correlate with proliferative activity? J. Nucl. Med., *42:* 721–725, 2001.
5. Shields, A. F., Grierson, J. R., Dohmen, B. M., Machulla, H. J., Stayanoff, J. C., Lawhorn-Crews, J. M., Obradovich, J. E., Muzik, O., and Mangner, T. J. Imaging proliferation *in vivo* with [F-18]FLT and positron emission tomography. Nat. Med., *4:* 1334–1336, 1998.
6. Sherley, J. L., and Kelly, T. J. Regulation of human thymidine kinase during the cell cycle. J. Biol. Chem., *263:* 8350–8358, 1988.
7. Machulla, H. J., Blocher, A., Kuntzsch, M., and Grierson J. R. Simplified labeling approach for synthesizing 3′-deoxy-3′-[^{18}F]fluorothymidine ([^{18}F]FLT). J. Radioanal. Nucl. Chem., *24:* 843–846, 2000.
8. Schmidlin, P. Improved iterative reconstruction using variable projection binning and abbreviated convolution. Eur. J. Nucl. Med., *21:* 930–936, 1994.
9. Hommura, F., Dosaka-Akita, H., Mishina, T., Nishi, M., Kojima, T., Hiroumi, H., Ogura, S., Shimizu, M., Katoh, H., and Kawakami, Y. Prognostic significance of p27^{KIP1} protein and ki-67 growth fraction in non-small cell lung cancers. Clin. Cancer Res., *6:* 4073–4081, 2000.
10. Dosaka-Akita, H., Hommura, F., Mishina, T., Ogura, S., Shimizu, M., Katoh, H., and Kawakami, Y. A risk-stratification model of non-small cell lung cancers using cyclin E, ki-67, and *ras* p21: different roles of G1 cyclins in cell proliferation and prognosis. Cancer Res., *61:* 2500–2504, 2001.
11. Harpole, D. H. Prognostic issues in non-small cell lung cancer. Chest, *107:* 267–269, 1995.
12. Apolinario, R. M., van der Valk, P., de Jong, J. S., Deville, W., van Ark-Otte, J., Dingemans, A. M., van Mourik, J. C., Postmus, P. E., Pinedo, H. M., and Giaccone, G. Prognostic value of the expression of p53, bcl-2, and bax oncoproteins, and neovascularization in patients with radically resected non-small cell lung cancer. J. Clin. Oncol., *15:* 2456–2466, 1997.
13. D'Amico, T. A., Aloia, T. A., Moore, M. B., Herndon, J. E., Brooks, K. R., Lau, C. L., and Harpole, D. H. Molecular biologic substaging of stage I lung cancer according to gender and histology. Ann. Thorac. Surg., *69:* 882–886, 2000.
14. Higashi, K., Ueda, Y., Yagishita, M., Arisaka, Y., Sakurai, A., Oguchi, M., Seki, H., Nambu, Y., Tonami, H., and Yamamoto, I. FDG PET measurement of the proliferative potential of non-small cell lung cancer. J. Nucl. Med., *41:* 85–92, 2000.
15. Vesselle, H., Schmidt, R. A., Pugsley, J. M., Li, M., Kohlmyer, S. G., Vallires, E., and Wood, D. E. Lung cancer proliferation correlates with [F-18]fluorodeoxyglucose uptake by positron emission tomography. Clin. Cancer Res., *6:* 3837–3844, 2000.
16. Brown, R. S., Leung, J. Y., Kison, P. V., Zasadny, K. R., Flint, A., and Wahl, R. L. Glucose transporters and FDG uptake in untreated primary human non-small cell lung cancer. J. Nucl. Med., *40:* 556–565, 1999.
17. Vansteenkiste, J. F., Stroobants, S. G., Dupont, P. J., De Leyn, P. R., Verbeken, E. K., Deneffe, G. J., Mortelmans, L. A., and Demedts, M. G. Prognostic importance of the standardized uptake value on (18)F-fluoro-2-deoxy-glucose-positron emission tomography scan in non-small cell lung cancer: an analysis of 125 cases. Leuven Lung Cancer Group. J. Clin. Oncol., *17:* 3201–3206, 1999.
18. Hicks, R. J., Kalff, V., MacManus, M. P., Ware, R. E., McKenzie, A. F., Matthews, J. P., and Ball, D. L. 18F-FDG PET provides high impact and powerful prognostic stratification in staging newly diagnosed non-small cell lung cancer. J. Nucl. Med., *42:* 1596–1604, 2001.
19. Mac Manus, M. P., Hicks, R. J., Ball, D. L., Kalff, V., Matthews, J. P., Salminen, E., Khaw, P., Wirth, A., Rischin, D., and McKenzie, A. F-18 fluorodeoxyglucose positron emission tomography staging in radical radiotherapy candidates with non-small cell lung carcinoma: powerful correlation with survival and high impact on treatment. Cancer (Phila.), *92:* 886–895, 2001.

Cancer Research
The Journal of Cancer Research (1916–1930) | The American Journal of Cancer (1931–1940)

3-Deoxy-3-[^{18}F]Fluorothymidine-Positron Emission Tomography for Noninvasive Assessment of Proliferation in Pulmonary Nodules

Andreas K. Buck, Holger Schirrmeister, Martin Hetzel, et al.

Cancer Res 2002;62:3331-3334.